



HAL
open science

The End of Einstein's Astronomy: Astronomical Origin for the Largest Marsquake Observed by InSight

Alexander N. Safronov

► To cite this version:

Alexander N. Safronov. The End of Einstein's Astronomy: Astronomical Origin for the Largest Marsquake Observed by InSight. 2024. <hal-04556936>

HAL Id: hal-04556936

<https://hal.science/hal-04556936v1>

Preprint submitted on 25 Apr 2024

HAL is a multi-disciplinary open access archive for the deposit and dissemination of scientific research documents, whether they are published or not. The documents may come from teaching and research institutions in France or abroad, or from public or private research centers.

L'archive ouverte pluridisciplinaire HAL, est destinée au dépôt et à la diffusion de documents scientifiques de niveau recherche, publiés ou non, émanant des établissements d'enseignement et de recherche français ou étrangers, des laboratoires publics ou privés.



Distributed under a Creative Commons CC BY 4.0 - Attribution - International License

2 The End of Einstein's Astronomy: Astronomical Origin for the 3 Largest Marsquake Observed by InSight

4 Alexander N. Safronov

5 Obukhov Institute of Atmospheric Physics, Russian Academy of Sciences, Pyzhevskii Per. 3,
6 119017 Moscow, Russia; email: safronov_2003@mail.ru; ORCID: 0000-0001-5960-6590

7 **Abstract:** In this study, we investigated the planetary configuration of the Solar system at the moment of the largest marsquake
8 s1222a observed by InSight. It is shown that the Solar system has a unique linear configuration formed by Saturn, Mars, Venus,
9 and Mercury. Also it was also found that during the 1222a marsquake (3:50 LMST) Mars was turned in the direction of Jupiter. It
10 has been suggested that the nature of this marsquake is the extrusion of gas through pingo chimneys or through cracks in the
11 Martian crust (sips) under the influence of external gravitational forces. Additionally, 18 more cases of marsquakes were ana-
12 lyzed. It was found that during marsquakes, planetary parallelism often took place, in which the planets line up in pairs parallel
13 to each other. It is assumed that possible sources of graviton may be not only planets, but also excited sites in the orbits of plan-
14 ets. It is shown that the excitation of the orbits of the planets is not arbitrary, but is determined by additional influence from other
15 planets. It has been found that gravitons can move both from the overlying orbits to the underlying ones, and in the opposite
16 direction. Several cases for the cascade transition of gravitons in a system of several orbits have been identified. These features
17 do not fit into the standard picture of Einstein's theory of relativity. Up-to-date astronomy is like the sinking of the Titanic.

18 **Keywords:** Mars; Marsquake; Planet Alignment; Planet Parallelism; Solar System Graviton
19

20 1. Introduction

21 The introduction should briefly place the study in a broad context and highlight why it is important. It should de-
22 fine the purpose of the work and its significance. The current state of the research field should be carefully reviewed
23 and key publications cited. Please highlight controversial and diverging hypotheses when necessary. Finally,
24 briefly mention the main aim of the work and highlight the principal conclusions. As far as possible, please keep the
25 introduction comprehensible to scientists outside your particular field of research. References should be numbered
26 in order of appearance and indicated by a numeral or numerals in square brackets—e.g., [1] or [2,3], or [4-6]. See the
27 end of the document for further details on references.

28 In the author's works [1] and [2] it was shown that seismic and volcanic activity on Earth can be activated by
29 planetary configurations. In particular, in [2], the geometry of the planets of the Solar system was studied during
30 strong earthquakes with a magnitude of more than 8 points (M_w8+) and occurring in the period from 1900 to 2011.
31 Three main planetary schemes were identified in which these strong earthquakes occurred, namely the generalized
32 Archimedes lever (gAL) pattern, the generalized Kepler conjunction (gKc) pattern, and the triangular pattern of the
33 remote cosmic signal detector (remote signal interceptor, cRS). Note that the cRS scheme is an analog of the LISA
34 experiment [3], however, instead of expensive satellites, which are not easy to accurately contain in a triangular
35 interference pattern, in our case the planets themselves line up at some point in time in a triangular pattern with a
36 resonant ratio of the distances between them. In [2] it was found that M_w8+ earthquakes occurred at 22 gAL, 42 gKc
37 and 28 cRS, which is 23.9 %, 45.7 % and 30.4 %, respectively, of the total number of cases studied. Therefore, it is of
38 interest to test the connection between marsquakes and planetary configurations. Some remarks about deep crisis in
39 the astronomy are presented in Section 5.

40 2. Materials and Methods

41 2.1. Strong marsquakes as studying object

42 On May 5, 2018 a special InSight (Interior Exploration using Seismic Investigations, Geodesy and Heat Transport)
43 mission was sent to Mars. The geophysical observatory successfully landed on Mars on November 26, 2018 in the

western region of Elysium Planitia at 4.5°N and 136.0°E. The InSight satellite includes the SEIS (Seismic Experiment for Interior Structure) seismometer package, which provides scientists with high-quality extra-terrestrial seismic data for the first time. For over the four years of the InSight mission, which ended on December 21, 2022, more than 1,300 events were recorded, see reviews [4], [5], and [6]. The InSight seismic event catalog is available from the IGP Data Center, NASA-PDS and IRISDMC, please see MSC dataset v14 [7] and an alternative catalog [8]. Marsquake features for martian days (sols) 0 – 478 (through the end of March 2020) can be found in [9], and for sols 0–1011, marsquake features covering events up to September 2021 can be found in [10]. In this work, we use Local Mean Solar Time (LMST) to determinate the diurnal cycle of marsquakes. Thus, the LMST 12-hour axis always points toward the Sun.

53 2.2. Astronomical data and method

To investigate the causes of strong marsquakes, we need to measure astronomical angles and distances between planets. This work used the Orbit Viewer Java applet from Osamu and Ron [11], which was created by Osamu Ajiki (AstroArts Inc.) in 1996 and modified by Ron Baalke (NASA/Jet Propulsion Laboratory, below JPL) in 2000–2001. Original Orbit Viewer is an interactive applet that displays the orbits of small bodies such as comets and asteroids in the Solar System in 3D projection. Orbits can be shown forward or backward. For example, a visualization of Comet 1P/Halley was presented in the JPL Small-Body Database Browser. For simplicity, all the figures below are presented in a 2D projection onto plane of the planet. In this projection, the direction of rotation of the planet is counterclockwise. The Orbit Viewer applet [12] is adapted for measuring the angles between the planets of the Solar System and determining the proportions in the positions of the planets. The following abbreviations were used in this study: Mercury: Mr, Venus: V, Earth: E, Mars: M, Jupiter: J, Saturn: S, Uranus: U, Neptune: N.

Planets located along the line are designated as $Planet_1$ - $Planet_2$ - $Planet_3$, in order of distance from the Sun. The angle (in degrees) between the three planets was calculated by placing the vertex of the angle on the more distant planet. For example, the linearity angle J-E-V is the smaller angle between the two lines JE and JV. During our exploration of planetary geometry, the alignment angle between the $Planet_i$ - $Planet_j$ and $Planet_j$ - $Planet_k$ lines was used, so this alignment angle α_{ijk} was defined in degrees as follows:

$$\alpha_{ijk} = 180^\circ / \pi \cdot \arccos \left(\frac{(R_{ij}^2 + R_{jk}^2 - R_{ik}^2)}{(2 \cdot R_{ij} \cdot R_{jk})} \right) \quad (1)$$

where i, j, k – three planets of the Solar System; x_i, y_i, z_i – the coordinates of the i – planet and the distance between the i and j planets are equal to $R_{ij} = \left((x_i - x_j)^2 + (y_i - y_j)^2 + (z_i - z_j)^2 \right)^{1/2}$. In connection with the search for an interference tracer, the notation of spatial relationships was used as the ration of distances between planets. This ratio was defined as:

$$N_{ij} = R_{i,j3} / R_{i3} \quad (2)$$

where $R_{i,j3}$ is the distance between the i, j planets to the Earth and $R_{j3} > R_{i3}$. We look for large interference extremes whose spatial ratio is close to integer values. Further, the designation that the line $Planet_1$ - $Planet_2$ is parallel to the line $Planet_3$ - $Planet_4$ is marked as symbol “||”, see Equation (3).

$$Planet_1 \ Planet_2 \parallel Planet_3 \ Planet_4 \quad (3)$$

76 3. Volcanic and seismic activity on Mars

77 3.1. Volcanic eruptions on Mars

As it is known that gaseous sulfur-containing compounds have never been detected in the Martian atmosphere, see, e.g. [13]. Let us recall that in the work Encrenaz et al. [13] to search for SO₂ in the atmosphere of Mars, the thermal spectrum of Mars at a wavelength of 7.4 μm, obtained by the Texas Echelon Cross Echelle Spectrograph (TEXES) at the NASA Infrared Telescope Facility (IRTF) is used. However, note that the sulfur-carrying molecules have been detected on the surface of Mars by the Viking lander, the Spirit and Opportunity rovers, and the OMEGA infrared spectrometer on board Mars Express, see [14, 15] and are mentioned therein.

Recall that astronomer N.A. Kozyrev from the Central Astronomical Observatory at Pulkovo in Russia was the first scientist who experimentally discovered lunar volcanism in 1958 [16, 17] and [18]. In the early morning of November 3, 1958, Kozyrev observed a volcanic eruption on the Moon near the central peak of the Alphons crater. First, dust was thrown out – volcanic ash, and then gases were released. During the eruption, the maximum emis-

sion was recorded at a wavelength of 4737 Å, which corresponds to the beginning of the Swan vibration band system of the carbon molecule C₂ (C₂H₂). The existence of C₂ was confirmed by the presence of other, but much weaker groups of Swan bands with maxima at 5165 and 5636 Å.

On Earth, unlike Mars and the Moon, seismic activity and volcanic eruptions occur mainly in the subduction zone, and gases containing sulfur compounds are released mainly during eruptions. In [1] it was shown that a ⁴⁰K nuclear layer at the boundary of the upper and lower mantle is the basis of the modern theory of seismology, volcanology, subduction and continental formation. Due to the presence of this hot nuclear layer at a depth of ~ 660 km, a thermopause is created, which separates light and heavy elements in accordance with Archimedes' law of buoyancy. Light elements float up, and heavy elements sink lower, into the deep layers of magma. That is why, with such vertical thermal stratification, volcanic lavas and ash plumes lack compounds containing heavy elements such as gold, platinum, silver and copper.

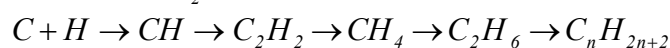
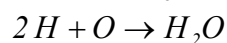
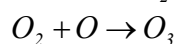
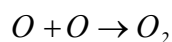
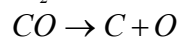
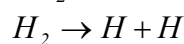
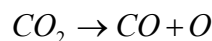
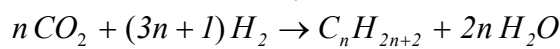
Therefore, when we talk about volcanism on planetary objects such as the Moon and Mars, we mean pseudo-volcanism, in which volcanoes emit precisely CO, CO₂, CH₄, C₂H₆, H₂O and C₂H₂, and not sulfur-containing compounds such as H₂S, SO₂ and SO₃, please see the corresponding section in [19], which described in detail the process of eruption of a lunar volcano. A more general overview of sedimentary volcanism on Mars can be found in [20].

3.2. Martian seismology activity and north-south dichotomy

Next, we will discuss the effect of dichotomy on marsquakes. Recall that the boundary between the northern lowlands and the southern highlands is usually called the North-South dichotomy in Martian geology. Marsquakes are observed mainly in the northern hemisphere of Mars, mainly near the equatorial dichotomy boundary please see [21], and data from the Mars Quake Service catalog (MQS v14) [7]. Nevertheless, the works mainly note the influence of dichotomy on the propagation of seismic waves and, accordingly, on the accuracy of localization of marsquakes (e.g. Kim et al. in [22]), and not on the process of formation of conditions for the occurrence of marsquakes themselves. Various hypothesis of the origin of the dichotomy boundary have been actively discussed, see e.g. [23,24,25]. A common opinion is that the dichotomy of the Martian hemisphere is formed as a result of an asteroid mega-impact.

At the same time, there is a strong impression that, according to a large group of researchers, planets can only collide with solid asteroids and meteorites, and not with comets. Comets, unlike asteroids, are made of ice, which evaporates when approaching the Sun, forming a characteristic comet tail. The gas composition of comet tails can vary, but in most cases comets are composed primarily of dry ice. The hypothesis about the possible collision of comets with planets is actively promoted by the author of this study. In particular, in [26] it was shown that a comet can break through the crust of protoplanets and explode inside them. Also about impact nuclear explosions, see [26-29], and about nuclear reactors inside planets, see Kuroda work in [30], and Herndon series of studies [31-35].

Note that a thermal nuclear explosion provides the formation of excess hydrogen (H) and deuterium (D). On the other hand, the original cometary gases CO₂ and nuclear hydrogen (H, D, H₂) provided secondary martian gases in the atmosphere and crust, such as CH₄, C₂H₆, C₂H₂ and others, through molecular (4) or atomic (5) channels the following chemical reactions:



The explosion of a comet inside a planet can lead to the formation of water H₂O and various radicals CH, CO, as well as second-order derivatives of the nuclear cycle containing nitrogen, such as -CN- and -NO-: NH₃, HCN, N₂O,

127 NO, NO₂ and N₂. For the chemical composition and gas forms of CH₄, CH₃OH, H₂CO, C₂H₆, C₂H₂, and C₂H₄ in the
128 Martian atmosphere, see also [36].

129 The creation of water H₂O and various hydrocarbon radicals under the Martian crust and in cracks leads to the
130 formation of water and gas-oil deposits in caverns, and the destruction of the crust occurs mainly in the northern
131 hemisphere of Mars. Let us also recall that the author of this study was the first to substantiate why oil and gas
132 deposits on Earth are more common in the northern hemisphere, while large diamond deposits dominate in the
133 southern hemisphere of the Earth, especially at the southern tip of Africa [26].

134 An alternative opinion about the origin of water on Mars reader will be able to find in [37-40], review [41] and
135 many others studies, referenced in them.

136 3.3. Seasonal and temporal behaviors of seismic activity on Mars

137 Judging by the absence of SO₂ in the atmosphere of Mars, it is clear that there is currently no active volcanism,
138 subduction or movement of lithospheric plates on Mars, so the probability of strong seismic events is very small,
139 and the magnitude of such a marsquake can be comparable to weak and very weak earthquakes. It was assumed
140 that the potential cause of marsquakes could be the following three factors: the movement of crustal blocks along
141 faults, the movement of magma along systems of cracks in the Martian crust, or the fall of large meteorites. There-
142 fore, it was a surprise to note the seasonal behavior of marsquake activity.

143 In [42,43] it was shown that solar declination is the most likely and the CO₂ cycle is the least likely driver of this
144 seismic activity. Although solar discrimination is weak, according to the authors of [42,43], solar declination and
145 CO₂ ice load are triggers for marsquakes. In this situation, we note that the largest number of marsquakes occur
146 nearby the Cerberus Fossae, the Grotta Valley, and only a few distant events were recorded near Olympus Mons
147 and in the Valles Marineris [4], [21] and InSight Marsquake Service Catalog (MSC v14) [7].

148 However, space images of the martian surface in these areas did not reveal thick ice sheets similar to the ice cover
149 of Greenland and Antarctica, which could lead to seismic movements of tectonic plates. This calls into question the
150 thesis that has been put forward that the icy load of CO₂ is the cause of marsquakes. Note that Knapmeyer et al. in
151 [42] also discussed the influence of meteorological conditions, daytime variations in surface temperature and wind,
152 as well as Phobos tide on the Martian seismic activity. So far, it has been shown that only two strong marsquakes,
153 s1000a and s1094b with magnitude M_w4.0 and 4.1, have been confirmed as impact-generated events [44] and [45].
154 Further, Fernando et al. [46] concluded that the largest marsquake, s1222a is of tectonic origin, but Lei and colleagues
155 in [47] suggested that some surface super-high-frequency marsquakes are of thermal origin.

156 Let's summarize everything written above. It can be stated that the activities of scientific groups studying
157 marsquakes have reached a dead end: on the one hand, marsquakes have been registered, but on the other, there is
158 no simple, clear and physically understandable explanation for this phenomenon.

159 3.4. Martian craters and pingos

160 It is well-known that water and gases such as CO₂, CH₄ trapped under the planet's crust could form a convex geo-
161 logical basin called pingos. In the geology of the Earth, pingos, methane craters and methane sips (outflow of gases
162 through cracks on the shelf), are well known. Some information on the creation, evolution and collapse of terrestrial
163 and Martian pingos can be found in [48, 49] and [50] and the references cited therein. Pingos can sometimes collapse
164 and form an reverse volcanic craters, which usually have the highest vertical walls and columns of chimneys, and
165 sometimes wells in the center of the craters [19]. Thus, it is easy to assume that the pseudo-volcanic activity, as well
166 as the activity of pingos and sips, leads to marsquakes and episodic methane emissions on Mars.

167 It is important to emphasize that there are many craters in the InSight landing area, which are gaseous pingos
168 craters, with collapsed pingos' domes. Externally, such Martian craters are similar to the same lunar gas craters,
169 have a rounded shape, high vertical walls, a depressed bottom and often a chimney in the middle of the crater, so
170 visually they are easy to distinguish from impact craters. It is important to note that in astronomy, craters are not
171 actually classified, that is, impact, pingos and the oldest original volcanic calderas are not distinguished. Thus, any
172 statistics based on crater counts may turn out to be unreliable, and studies using a dating method based on such
173 statistics are clearly pretentious and dogmatic in nature.

174 So let's get back to discussing the problems of marsquakes. It can be assumed that the external gravitational load
175 on Mars leads to the squeezing out of carbon dioxide, methane and water vapor through the chimneys of ping
176 craters, cracks in the crust and gas sips. Then the seasonality and daily variations of marsquakes are easily ex-
177 plained by the freezing of gases and water when passing through such pipes (black smokers or chimneys). Ac-

178 cording to this hypothesis, maximum seismic activity should be achieved in spring and summer and mainly im-
 179 mediately after sunset, when the thickness of the ice plug is not yet large. A small external gravitational influence
 180 leads to an increase in pressure in geological cavities filled with gases. The effect of knocking out the ice plug
 181 blocking the chimney of pingos craters and crustal cracks is similar to knocking the cork out of a champagne bottle
 182 when shaken.

183 On the other hand, the studies of marsquakes give us a unique opportunity to observe the process of graviton
 184 formation in the Solar System. Thus, the purpose of this work is to test the connection between external gravita-
 185 tional load and marsquakes.

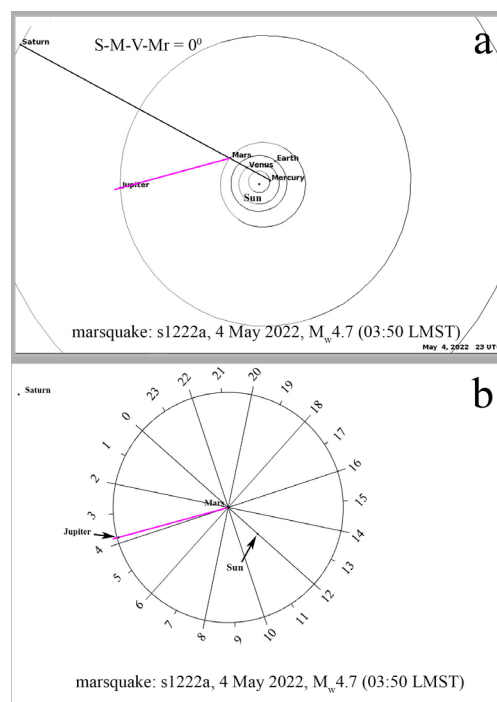
186 4. Results

187 4.1. The strongest s1222a marsquake

188 The strongest s1222a marsquake occurred on May 4, 2022 at 23:23:07 UTC, early Martian morning at 03:54:39 LMST
 189 (Local Mean Solar Time). The magnitude of this marsquake was $M_w 4.7$. This event occurred within an almost ellipse
 190 with an epicenter of about 3.0°S , 171.9°E at ~ 2200 km from InSight [46, 51]. The configuration of the planet corre-
 191 sponding to the moment of the marsquake 1222a is shown in Figure 1. This configuration is unique and is charac-
 192 terized by 4-planet alignment, i.e. four planets located in the Saturn–Mars–Venus–Mercury line, please see the black
 193 line in Figure 1a.

194 Figure 1b shows the polar axis of the Local Mean Solar Time (LMST). It is assumed that the 12h-LMST axis is
 195 always directed towards the Sun. The purple lines in Figures 1a and 1b correspond to the directions of the LMST.
 196 Thus, the purple line is the LMST-line, which characterizes the self rotation of Mars. The LMST-line helps us iden-
 197 tify the source of the gravitational signal (vortexes, gravitons). In this case under study, 1222a graviton probably
 198 arrived on Mars from Jupiter. Thus, we present the main conclusion of this study about the astronomical origin of
 199 the largest marsquake observed by InSight. Note that in [46] it is written about the tectonic origin for this
 200 marsquake.

201 Researchers studying marsquakes are professional astronomers and astrophysicists, not classical geologists and
 202 geophysicists who rarely pay attention to the starry sky. The reason why none of them paid attention to the con-
 203 nection between the marsquakes and the state of the Solar System remains a mystery. Either they did not pay
 204 enough attention to this, which is well-known in science as a paradox of “*Invisible Gorilla*” [52], or they wanted to
 205 remain ideologically tolerant, see the hard discussion in Section 5.
 206



207
 208 **Figure 1.** The planetary configuration for the strongest s1222a marsquake (May 4, 2022,
 209 23:23:07 UTC, 03:54:39 LMST), whose magnitude was $M_w 4.7$, is presented. (a) – the alignment

of Saturn–Mars–Venus–Mercury at 23 UTC is shown by a black line; (b) is the polar axis of the Local Mean Solar Time (LMST). It is assumed that the 12h-LMST axis always directed to the Sun, please see Figure 1b. The purple lines in Figures 1a and 1b correspond to the directions of the LMST, i.e. they probably determine the source of gravitational signal (vortexes, gravitons). Thus, the purple line is the LMST-line, which characterizes the self-rotation of Mars. In this case under study, graviton came to Mars from Jupiter.

4.2. The planet alignments and strong marsquakes

In previous works by the author [1, 2] and [19], it was shown that the excitation of the Solar system can occur due to the linearization of planets, historically called planetary alignment or Kepler's conjunction. Therefore, according to the principle of connecting the lever of Archimedes and Kepler, the Third Law of Motion should be changed by adding a few words to the end of the text of the law:

“When one body exerts a force on a second body, the second body exerts a force equal in magnitude and opposite in direction to that of the first body in the absence of obstacles in the path between these bodies” (6)

Alignments of planets that are registered for two marsquakes (s0802a, s0809a) are presented in Figure 2. Note that in both these cases the alignment of the planets is the same: the linearization of Jupiter-Mercury-Earth. Then the continuation of the LMST-lines (purple lines) at 23:09 and 23:34 LMST pass through the position of Mercury. Thus, we could assume that gravitational vortexes originate from Mercury.

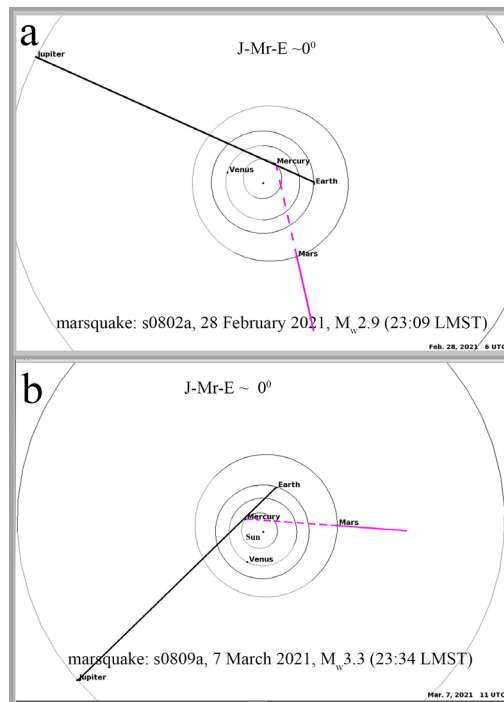
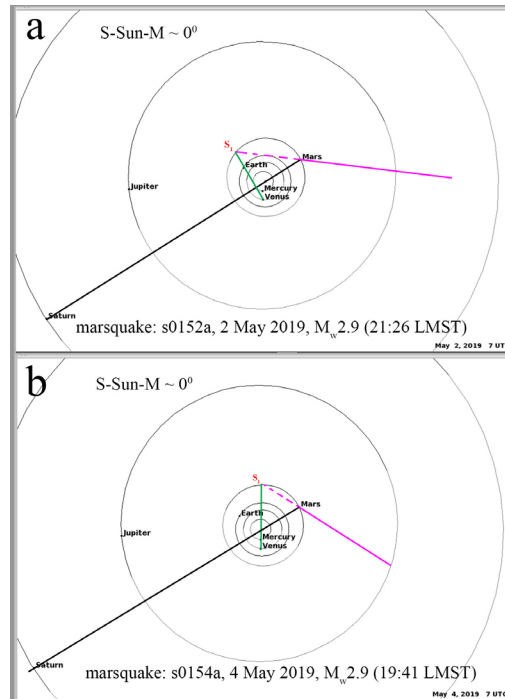


Figure 2. The same planetary alignments (Jupiter–Mercury–Earth) were recorded for two marsquakes (s0802a, s0809a). Note that in both these cases, the continuations of the LMST-lines (purple lines) at 23:09 and 23:34 LMST pass cross through position of Mercury. The purple lines are the LMST-lines that characterize the self-rotation of Mars.

In the following Figures 3 and 4, we have demonstrated that the sources of vortexes (gravitons) can be activated areas of the orbits of Mars and Jupiter. Two marsquakes (s0152a, s0154a) that occurred on May 2 and 4, 2019 and took place at the Saturn-Sun-Mars alignments are shown in Figures 3a and 3b. In both cases, gravitational signals (vortexes, gravitons) came to Mars from sections of the orbit of Mars itself, marked as a virtual source S1. However, on May 2, 2019, the excitation of the orbit of Mars occurred due to the impact of Earth and Venus, please see green line in Figure 3a. However, on May 4, the excitation of the orbit of Mars, see site S1, was determined by the position of the planets Venus, Mercury and probably the Sun, now please pay attention to the green line in Figure 3b.

238 The planetary configurations of the s0189a and s0475a marsquakes are shown in Figures 4a and 4b. The planet
 239 alignments are shown by black lines. In these Figures, we demonstrate that the orbital sites (virtual source S_1) were
 240 activated in the orbit of Jupiter as a result of the impact of the Venus–Sun linearization, please see the green lines in
 241 Figures 4a and 4b. Thus, in both cases s0189a and s0475a, gravitational vortexes came to Mars due to disturbed sites
 242 of the upper laying planet, Jupiter.
 243



244

245

246

247

248

249

250

251

Figure 3. Two marsquakes (s0152a, s0154a) are presented, which occurred on May 2 and 4, 2019 and have Saturn-Sun-Mars alignments. The alignments of the planets are shown by black lines. In both cases, gravitational signals (vortexes, gravitons) came to Mars from parts of the orbit of Mars itself, marked as a virtual source S_1 . On May 2, 2019, the excitation of the orbit of Mars occurred due to the impact of Earth and Venus, please see the green line in Figure (a). However, on May 4, the excitation of the orbital S_1 site was determined by the position of the planets Venus, Mercury and, probably, Sun, see the green line in Figure (b).

252

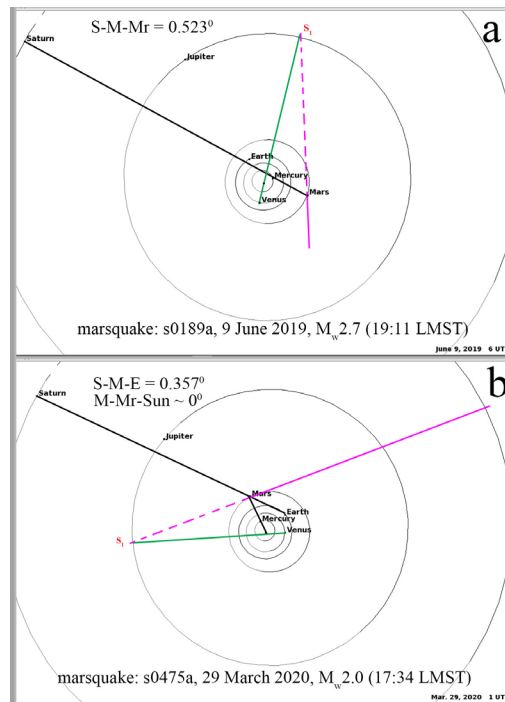


Figure 4. The planetary configurations for the cases of marsquakes s0189a (Figure a) and s0475a (Figure b) are presented. The planet alignments are shown by black lines. The purple lines are the LMST-lines that characterized self-rotation of Mars. In these Figures, we demonstrate how the linearity of Venus–Sun disturbs the orbit of Mars, please see the position of the virtual source S_1 .

4.3. Planetary parallelism and marsquakes

Earlier in the author's work [2] it was discovered that in addition to the resonant triangular schemes of eLISA, the processes of perturbation of the Solar system can also be caused by planetary parallelism (PP). The planetary principle is similar to the Fabry–Perot interferometer in optics. Therefore, it is worth paying attention to the presence of parallelism of planets during marsquakes.

First, we demonstrate planetary parallelism (PP) on the planet configurations of marsquakes (s0133a, s0173a), please see Figures 5a and 5b. Planetary parallelisms are highlighted with parallel blue lines and blue labels. For the s0133a marsquakes, it was recorded that the Jupiter–Venus line is in parallel of Earth–Mars line (JV || EM) and for s0173a) in the Jupiter–Venus line is in parallel to the Sun–Mercury line (JV || SunMr).

In the both studied cases, these were the activation sites of Marian's orbit. In Figure 5a it is shown that the site of the Mars' orbit was under the pressure of the Venus–Mercury linearity, and Figure 5b shows that the Mars site was under the pressure of the Earth–Venus linearity, please see the green lines. However, no planetary alignments have been detected, so it is possible that the Solar system is reacting to an external galactic influence or Solar system was activated for another unknown reason.

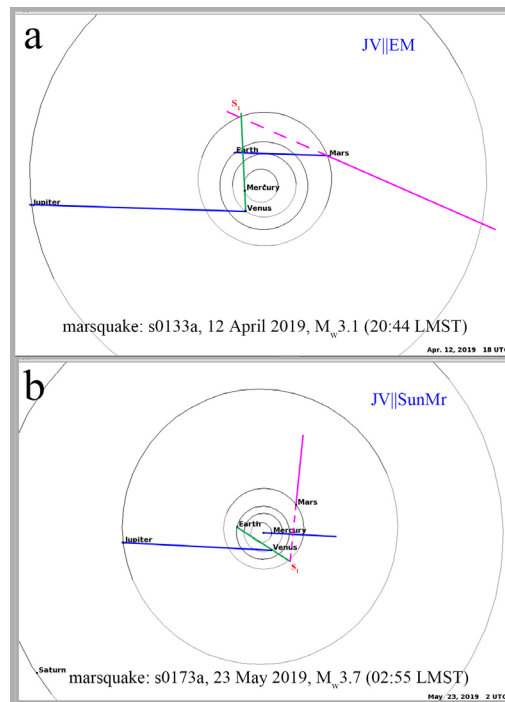


Figure 5. Planetary parallelism (PP) was demonstrated on the planet configurations of marsquakes (s0133a, s0173a). The planetary parallelism is highlighted by parallel blue lines and blue labels. (a) – The Jupiter–Venus line is parallel to the Earth–Mars line (JV||EM); (b) – the Jupiter–Venus line is parallel to the Sun–Mercury line (JV||SunMr). Both Figures (a, b) show that the activation of the Martian orbits took place in the intervals marked red labels S1. In Figure (a), the orbit of Mars was under the pressure of the Venus–Mercury linearity, and in (b) the orbit of Mars was under the pressure of the Earth–Venus linearity, please see the green lines. The alignment of the planets has not been detected, so it is possible that the solar system is reacting to an external galactic influence. The principle of planetary parallelism is similar to the Fabry–Perot interferometer in optics.

Next, we will give a couple more examples of planetary parallelism (PP), but in these studying cases the orbits of far planets could be involved in process of graviton emissions. In Figure 6a, the Jupiter–Venus line is parallel to the Mercury–Sun line (JV||MrSun), and in Figure 6b, the Jupiter–Mars line is in parallel to the Earth–Mercury line (JM||EMr). At the moment s0128a marsquake, the graviton source is probably located in the orbit of Jupiter (Figure 6a), but the activated site for s0185a marsquake is located in the orbit of Saturn (Figure 6b). The reasons for the activation of the orbit are the same, it is the Earth–Venus linearity, please see the green lines.

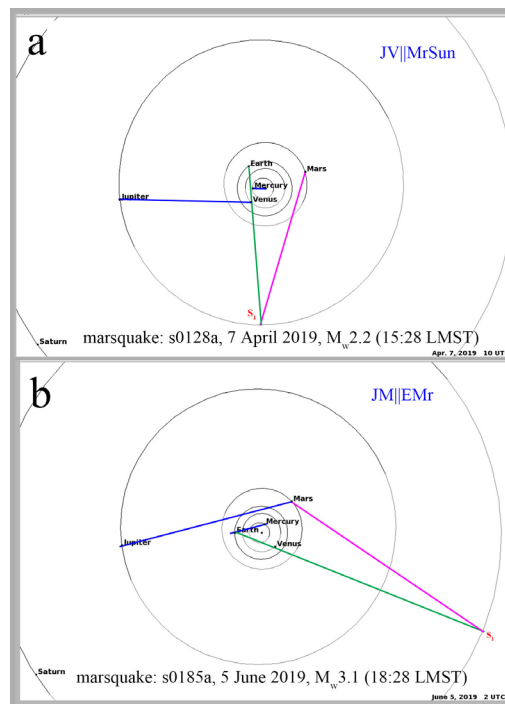


Figure 6. The orbits of distant planets could be involved in the process of gravitonic emissions in two examples (s0128a, s0185a) of marsquakes: in Figure (a) – S_1 source is, probably, located in the Jupiter orbit, in (b) – in the Saturn orbit. The activation of the orbit is the same, this is the Earth–Venus line, please see the green lines. However, the schemes of planetary parallelism PP (blue lines) are different: in Figure (a) – Jupiter–Venus is parallel to Mercury–Sun (JV||MrSun), in Figure (b) – the Jupiter–Mars line is parallel to the Earth–Mercury line (JM||EMr).

Further, we demonstrate multiple planetary parallelisms on the planetary configurations of the s0421b and s1022a marsquakes. In these cases of study, we pay attention to the fact that the sources of graviton (S_1) could be involved in the PP process. For the marsquakes s0421b, it was recorded that Mars–Earth is parallel to Mercury–Venus, and Jupiter–Mars is parallel to Earth– S_1 (Figure 7a). For the s1022a marsquake the Jupiter–Mercury line is parallel to Earth– S_1 , and Earth–Venus is parallel to Mars– S_1 (Figure 7b).

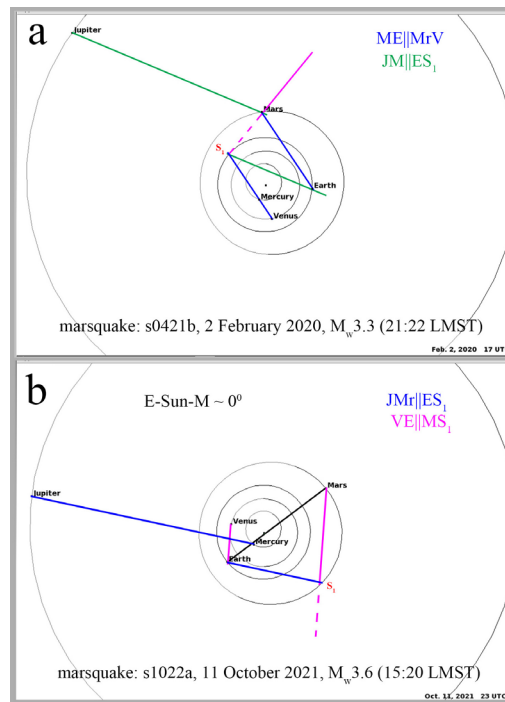


Figure 7. We once again demonstrate planetary parallelism (PP) on the planetary configurations of the marsquakes s0421b and s1022a. However, in these studied cases, we draw attention to the fact that the sources of gravitons (S_1) could be involved in the PP process. The LMST-lines are drawn with purple lines; the planetary parallelism (PP) is highlighted with blue lines. In addition, in Figure (b), the alignment of the Mars-Sun-Earth planets is drawn with a black line.

4.4 Cascading perturbations of planetary orbits

In the course of this study, cases of cascading disturbances of the orbits of planets were also discovered. This may correspond to the cascade transition of the graviton from one orbit to another before it reaches the surface of Mars. Below are several cases of such cascading transitions.

The s0235b marsquake, which occurred on July 26, 2019 with a magnitude of $M_w 3.7$, has the planet configuration shown in Figure 8a. The orbital sites involved in the graviton generation process are marked with red labels S_1 and S_2 . These sites have been activated by the Venus–Mars planet parallelism system ($JS_1 || ES_2 || VM$), please see the green lines in Figure 8a. Thus, it can be concluded that the cause of this marsquake was a graviton that passed along the purple line: $S_2 \rightarrow S_1 \rightarrow Mars$. Figure 8b shows the configuration of the planet during the s0794a marsquake. This marsquake occurred on February 19, 2021 with a magnitude of $M_w 3.1$. In the case of the study of the s0794a marsquake, the graviton jumps from the lower orbits to the upper ones: $Earth \rightarrow Mercury \rightarrow Mars$ along the margin line: $S_2 \rightarrow S_1 \rightarrow Mars$. The parallelism of the planets in this case is as follows: The Mercury – Earth line is parallel to the Venus–Sun line. Note that no alignment of the planets was detected in this marsquake, so again it can be assumed that the Solar System reacts to external influences.

More complex events of cascade excitations of orbital sites that took place during the s0183a and s0343b marsquakes are demonstrated in Figures 9a and 9b. The planetary parallelism in the Figures is highlighted in blue; the lines of orbital excitation are drawn in green; the sources of graviton vortexes are designated as S_1 and S_2 ; the LMST-line is colored purple. Cascading transitions are also shown in Figures S6a and Figure S9b in the Supplementary. However, please note that the interpretation of jumping gravitons is not as simple as it might seem at first glance.

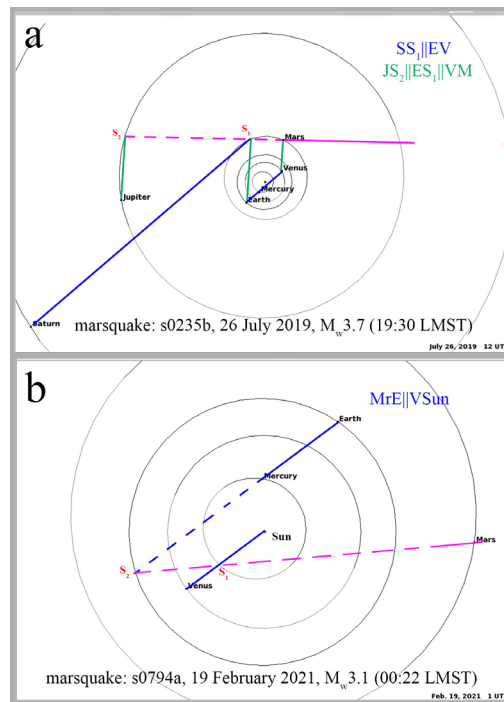


Figure 8. The cascade transition of gravitons between the orbits of planets is represented by two cases: (a) – the s0235b marsquake, which occurred on July 26, 2019 with a magnitude of $M_w 3.7$, and (b) – the s0794a marsquake, which occurred on February 19, 2021 with a magnitude of $M_w 3.1$. The orbital sites involved in the process of generating gravitons are marked with red marks S_1 and S_2 . The planetary parallelism (PP) is marked with blue and green lines. The LMST lines are highlighted in purple. The alignment of the planets was not detected, so again it can be assumed that the Solar system reacts to external influences.

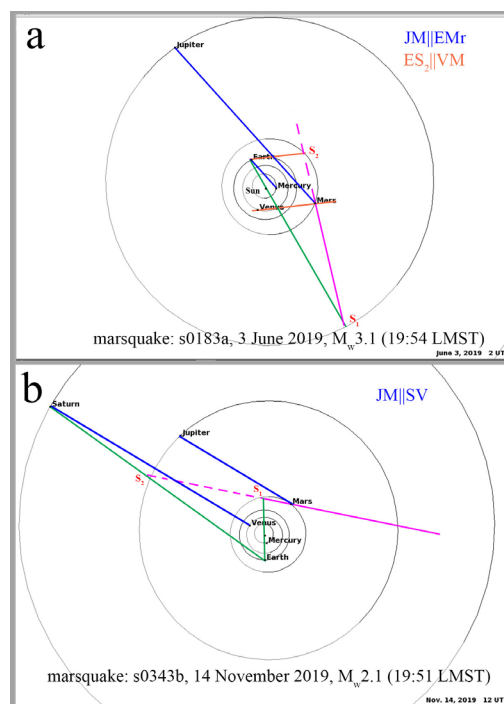


Figure 9. The cascade excitations of the orbital sites that occurred during the marsquakes s0183a (Figure a) and s0343b (Figure b) are demonstrated; please see the red marks S_1 and S_2 . The

planetary parallelism is highlighted in blue; the lines of orbital excitation are drawn in green; the LMST-lines are colored purple; the sources of graviton vortexes are labeled as S_1 and S_2 .

4.5. Summary

We have considered several characteristic configurations of planets that took place during marsquakes. The influence of planetary alignments, planetary parallelisms, and the possibility of cascading gravitonic transitions between planetary orbits were shown. To be convincing, we will once again demonstrate the variability of the causes of graviton generation in the Solar System. In Figures 10a and 10b we demonstrate that the sources of gravitons a planet (Figure 10a) as well as several sites of executed planetary orbits (Figure 10b). The configurations shown correspond to the s0234c and s0976a marsquakes, which occurred on July 25 and August 25, 2021 at 20:46 and 02:20 LMST. All the planetary parameters for the 19 marsquakes studied in the work are summarized in Table 1.

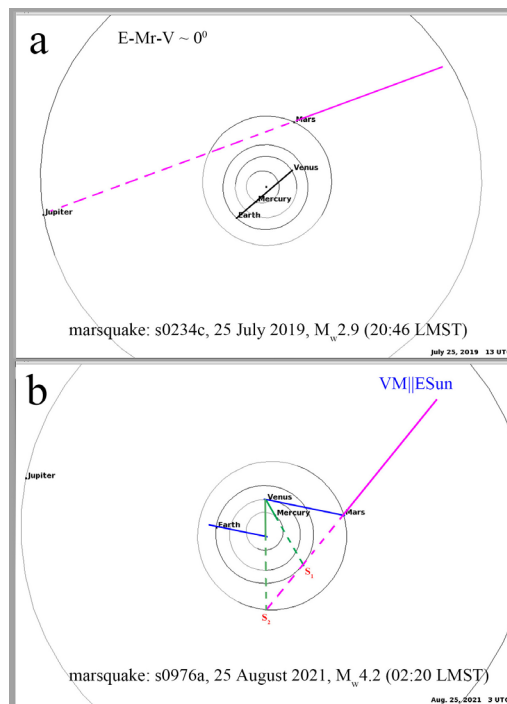


Figure 10. Two marsquakes (s0234c, s0976a) occurred on July 25 and August 25, 2021 at 20:46 and 02:20 LMST. In these examples, we demonstrate once again that the sources of gravitons can be planets (Figure a), as well as several active sites (S_1 , S_2) of planetary orbits (Figure b).

Table 1. A summary list of parameters for the 19 selected marsquakes. LMST stands for Local Mean Solar Time (Martian local time), and UTC stands for Greenwich terrestrial time. The "Type" of the marsquake is associated with the recorded seismic frequencies, so the abbreviations of type are as follows: Broad Band (BB), Low Frequency (LF), High Frequency (HF), and Very High Frequency (VHF) events. The parameter "Quality" is described in the MSC V14 Guide (2023). A description of the parameter "Magnitude" can be found in [53].

Figure	Name	Magnitude	Date	UTC	LMST	Quality	Type	Alignment	Parallelism	Initialization	Source
1a	s1222a	M4.6	2022-05-04	23:23:07	03:50	A	BB	S-M-V-Mr	-	-	planet J
2a	s0802a	M2.9	2021-02-28	06:07:21	23:09	B	BB	J-Mr-E	-	-	planet Mr
2b	s0809a	M3.3	2021-03-07	11:09:26	23:33	A	LF	J-Mr-E	-	-	planet Mr
3a	s0152a	M2.9	2019-05-02	07:19:57	21:26	C	BB	S-Sun-M	-	V-E	orbit M

3b	s0154a	M2.9	2019-05-04	07:03:35	19:41	C	BB	S-Sun-M	–	V-Mr-Sun	orbit M
4a	s0189a	M2.7	2019-06-09	05:35:56	19:11	B	LF	S-Mr-M	–	V-Sun	orbit J
4b	s0475a	M2.0	2020-03-29	00:37:59	17:34	B	VHF	S-M-E, M-Mr-Sun	–	V-Sun	orbit J
5a	s0133a	M3.1	2019-04-12	18:00:20	20:44	C	BB	–	JV EM	V-Mr	orbit M
5b	s0173a	M 3.7	2019-05-23	02:19:10	02:55	A	LF	–	JV SunMr	E-V	orbit M
6a	s0128a	M2.2	2019-04-07	09:31:52	15:28	B	VHF	–	JM MrSun	E-V	orbit J
6b	s0185a	M3.1	2019-06-05	02:06:38	18:28	B	BB	–	JM EMr	E-V	orbit S
7a	s0421b	M3.3	2020-02-02	16:42:33	21:22	C	LF	–	ME MrV	JM ES ₁	orbit E
7b	s1022a	M3.6	2021-10-11	23:14:29	15:20	A	LF	M-Sun-E	–	JMr ES ₁ , VE MS ₁	orbit M
8a	s0235b	M3.7	2019-07-26	12:15:39	19:30	A	BB	–	–	SS ₁ EM, JS ₂ VM	orbits J, M
8b	s0794a	M3.1	2021-02-19	01:21:17	00:22	B	VHF	–	MrE VSun	–	orbits E, Mr
9a	s0183a	M3.1	2019-06-03	02:22:02	19:54	B	LF	–	JM EMr	E-Sun, ES ₂ VM	orbits M, J
9b	s0343b	M2.1	2019-11-14	11:57:48	19:51	B	HF	–	SV JM	E-Sun, E-S	orbits M, J
10a	s0234c	M2.9	2019-07-25	12:46:45	20:45	C	LF	E-Mr-V	–	–	planet J
10b	s0976a	M 4.2	2021-08-25	03:32:20	02:20	A	LF	–	VM ESun	MrSun MS ₁	orbits M, E

5. Planet geometry and Einstein's General Theory of Relativity

Since in this work discusses effects related to planetary geometry, we should pay some attention to considering this issue. Note that Albert Einstein was not the first to explore the connection between geometry and astronomy. As it is known, ancient philosophers and mathematics such as Moses, Thales, Pythagoras, Plato, Archimedes, Aristotle and Hypatia studied the relationship between natural processes and the geometry of the planets. Albert Einstein was a poorly educated person, so in his publications you will not find any references to the works of ancient philosophers and mathematicians, or to the works of astronomers of the 17th and 18th centuries, in particular to the related works of Kepler, Bode, Titius, and Laplace.

When we talk about the geometry of planets, we first of all think about the linearization of the position of the planets. In different periods of the development of science, this linearization of the planets has been called the Orion belt (Moses), Music Theory (Pythagoras), harmony of the spheres (Plato, Aristotle, Theon), planet lever (Archimedes), Kepler's conjunction (Kepler), "*Jupiter Effect*" (Gribben and Plagemann), and planet alignment (Mörner and colleges).

Moreover, the orbital resonance is also relevant to the geometry of the planets. So, Laplace first drew attention to the orbital resonance of Jupiter's satellites Ganymede, Europa and Io in a ratio of 1:2:4, when two Io-Europa conjunctions and four Io-Ganymede conjunctions occur during the rotation of the satellites around Jupiter. Since the orbital resonance is characterized by a ratio of integer values, it is sometimes called the numerology of planets. Therefore, it is impossible to separate the geometry of the planets (planet linearization / Kepler conjunction / planet alignment) from the numerology of the planets. It is important to note that a number of journals (Nature, Icarus, A&A journal, Copernicus) have banned the publication of the works by Kepler, Bode and Titius.

However, recently new methods have been developing rapidly and successfully in exoplanetary astronomy. Thus, the use of the astro-combs method gave an impetus to the study of exoplanets of remote stars. Analysis of the location of exoplanets revealed the presence of orbital resonances in many stellar systems. In particular, a long sequence of resonant frequencies was detected in the planetary systems HD 110067, TOI-178 and TRAPPIST-1 [54, 55] and [56]. Some new information about exoplanets could be found in [57] and [58]. Please note that the above-mentioned features of the alignment or connection of the planets in no way fit into the framework of Einstein's general theory of relativity. In fact, the works Luger et al., Leleu et al. and Luque et al. [54, 55] and [56] are an important milestone in the unconditional decline of Einstein's theory of relativity.

To summarize. The results of [54–56], as well as the classic works of Pierre-Simon de Laplace, Johannes Kepler, Johann Elert Bode, and Johann Daniel Titius and previous studies in which a report on the influence of planetary configurations on seismic activity [1, 2, 59-61], on solar activity [62-68], and on climate processes [69-71] question the fundamental modern postulates of astronomy.

The main opponents of my studies are supporters of Albert Einstein's theory. Billions of dollars were spent on substantiating Albert Einstein's theory of gravity. However, the ambiguous results obtained by the LIGO and VIRGO teams give reason to believe that the general theory of relativity, developed in the last century by Albert Einstein, is incorrect. The joint work of LIGO, Virgo and KAGRA reported that 35 gravitational wave events were detected between November 2019 and March 2020, 32 of which were most likely mergers of black holes (mBH), in which two black holes spiral around each other and finally join together, the event, which emits a gravitational wave burst by GWTC-3 Team (2023) [72]. Thus, these Teams detect regular collisions of 3 mBH for two weeks. It is not any evidence of such regular mBH collisions. Note that this frequency is more similar to the frequency of bursts at shale gas mining or other anthropogenic activities than to the gravitational tsunami from black hole collisions.

An attempt to identify the sources of gravitational waves has led to searching mBH events and finally a revision of the concepts of dark matter and dark energy. As it is well-known Adam Riess, a physicist at Johns Hopkins University, recently said in Baltimore: *"With measurement errors negated [between James Webb Space Telescope (JWST) and Hubble Space Telescope measurements], what remains is the real and exciting possibility we have misunderstood the universe"*, please also see the discussion in [73]. Remark that A. Riess holds a Nobel Prize for co-discovering the fact that the universe's expansion is accelerating, due to a mysterious phenomenon now called *"dark energy"*. In 2023 the European Space Agency launched a special Euclid mission, aiming to produce a cosmic map of dark matter. The future of this mission looks blurry and uncertain.

In frame of the dark matter crisis, two alternative theories have appeared that deny the existence of dark matter [74, 75]. The interpretation of gravity proposed by Oppenheim and Rousseau would allow describing some phenomena without resorting to concepts such as dark energy and dark matter. Let's draw readers' attention to the statement of Oppenheim and Russo, who wrote in [74]: *"The gravity has a long history of being a trickster. The dark matter nature has remained mysterious and searches by the Large Hadron Collider have come up empty-handed. In the absence of any direct evidence for dark energy or dark matter it is natural to wonder whether they may be unnecessary scientific constructs like celestial spheres, ether, or the planet Vulcan, all of which were superseded by simpler explanations"*.

Therefore, we push reader to understand the very simple and clear fact that that in nature it is not reasonable arguments to write the space-time relation, which usually described in modern cosmology by the Friedmann–Lemaître–Robertson–Walker (FLRW) metric, as following:

$$\begin{aligned} ds^2 &\equiv g_{\mu\nu}x^\mu x^\nu = a^2(\eta)[d\eta^2 - dx^2] \\ dt^2 &\equiv a^2(\eta)d\eta^2 \end{aligned} \quad (7)$$

where $g_{\mu\nu}$ is the metric tensor, a is a scale factor describing the expansion or contraction of space, and η is conformal time. An error in axiomatic is fatal, so up-to-date astronomy is like the sinking of the Titanic.

All above remarks indicate that it is the end of the Einsteinian era. Unfortunately, the author is forced to report that nuclear astrophysics, like astronomy, does not stand up to the stress test, please see discussion in [76].

6. Conclusions

In this study, we investigate the planetary configuration corresponding to the moment of the largest marsquake s1222a observed by InSight. It is shown that this marsquake corresponds to a unique linear configuration formed by Saturn, Mars, Venus, and Mercury. At the moment of a marsquake, the angle between these planets is zero, up to the accuracy of the orbit calculation method, the discreteness of which is 1 hour. Additional research has shown that during the earthquake on Mars, which occurred at 03:50 LMST (Martian time), Mars was turned towards Jupiter. It has been suggested that the nature of this marsquake is squeezing of gas through chimneys of pingos or crust cracks under the influence of external gravitational forces.

In addition to this case, 18 more cases of marsquakes were analyzed, in which it was shown that the external gravitational influence can be enhanced by parameters such as the planet alignments, as well as the parallelism of the planets. It has been shown that possible sources of gravitons can be not only planets, but also excited sites of the planetary orbits. It is found that the excitation of the sites of the orbits of the planets is not arbitrary, but is determined by additional influence from other planets.

Thus, thanks to the study of marsquakes, the complex nature of the generation of gravitons of the Solar system was revealed. It has been shown that gravitons can move both from higher orbits to lower ones and in the opposite direction. Several cases of cascading transition of gravitons in a system of several planetary orbits have been identified. It should be particularly noted that the discovered patterns do not fit into the standard picture of Einstein's theory of relativity.

Supplementary Materials: The following supporting information can be downloaded at: www.mdpi.com/xxx/s1, Table S1: The list of parameters for 11 more marsquakes; Figure S1: The configuration of the planets during the s0784a and s1102a marsquakes; Figure S2: The configuration of the planets during the s0756a and s0923d marsquakes; Figure S3: The parallelism of the planets during the s0864a and s1048d marsquakes; Figure S4: Detailed configurations of the planets in the s0105a marsquake; Figure S5: A detailed configuration of the planets for the (s0290b) marsquake; Figure S6: A configuration of the planet for the (s0734a) marsquake; Figure S7: The detailed planetary configuration for the (s1133c) marsquake; Figure S8. One more detailed planetary configuration for (s0820a) marsquake.

Author Contributions: Alexander N. Safronov designed the study, analyzed the data, made model simulations and wrote the manuscript.

Funding: This research received no external funding.

Acknowledgments: The author gratefully acknowledges colleagues and my wife for suggesting the topic of this paper and for the very thorough revision of the manuscript.

Conflicts of Interest: The author declares no conflicts of interest.

References

1. Safronov, A.N. New Theory of Effusive and Explosive Volcanic Eruptions. *International Journal of Geosciences* **2022**, *13*, 115-137, doi:10.4236/ijg.2022.132007
2. Safronov, A.N. Astronomical Triggers as a Cause of Strong Earthquakes. *International Journal of Geosciences* **2022**, *13*, 793-829, doi:10.4236/ijg.2022.139040.
3. Bayle, J.-B.; Bonga, B.; Caprini, C.; Doneva, D.; Muratore, M.; Petiteau, A.; Rossi, E.; Shao, L. Overview and progress on the Laser Interferometer Space Antenna mission. *Nat Astron* **2022**, *6*, 1334-1338, doi:10.1038/s41550-022-01847-0.
4. Giardini, D.; Lognonné, P.; Banerdt, W.; Pike, W.; Christensen, U.; Ceylan, S.; Clinton, J.F.; van Driel, M.; Stähler, S.C.; Böse, M., et al. The seismicity of Mars. *Nature Geoscience* **2020**, *13*, 205-212, doi:10.1038/s41561-020-0539-8.
5. Duran, C.; Khan, A.; Ceylan, S.; Zenhausern, G.; Stähler, S.; Clinton, J.F.; Giardini, D. Seismology on Mars: An analysis of direct, reflected, and converted seismic body waves with implications for interior structure. *Physics of the Earth and Planetary Interiors* **2022**, doi:10.1016/j.pepi.2022.106851.
6. Lognonne, P.; Banerdt, W.B.; Clinton, J.; Garcia, R.F.; Giardini, D.; Knapmeyer-Endrun, B.; Panning, M.; Pike, W.T. Mars seismology. *Annual Review of Earth and Planetary Sciences* **2023**, *51*, doi:10.1146/annurev-earth-031621-073318.
7. MSC dataset v14. Mars Seismic Catalogue (MSC) V14 2023-04-01, supported by InSight Marsquake Service, InSight Mission. ETHZ, IPGP, JPL, ICL, University of Bristol. **2023**, doi:10.12686/a21.
8. Dahmen, N.L.; Clinton, J.F.; Meier, M.-A.; Stähler, S.C.; Ceylan, S.; Kim, D.; Stott, A.E.; Giardini, D. MarsQuakeNet: A more complete marsquake catalog obtained by deep learning techniques. *Journal of Geophysical Research: Planets* **2022**, *127*, e2022JE007503, doi:10.1029/2022JE007503.
9. Clinton, J.; Ceylan, S.; van Driel, M.; Giardini, D.; Stähler, S.; Böse, M.; Charalambous, C.; Dahmen, N.L.; Horleston, A.; Kawamura, T., et al. The Marsquake catalogue from InSight, sols 0–478. *Physics of the Earth and Planetary Interiors* **2021**, *310*, 106595, doi:10.1016/j.pepi.2020.106595.
10. Ceylan, S.; Clinton, J.F.; Giardini, D.; Stähler, S.C.; Horleston, A.; Kawamura, T.; Bose, M.; Charalambous, C.; Dahmen, N.L.; van Driel, M., et al. The marsquake catalogue from InSight, sols 0–1011 *Physics of the Earth and Planetary Interiors* **2022**, *333*, 106943, doi:10.1002/essoar.10512032.1.
11. Osamu, A.; Ron, B. Osamu Ajiki 1996, Ron Baalke, 2000-2001, "OrbitViewer Applet". <http://www.astroarts.jp/products/orbitviewer/OrbitViewer-1.3.tar.gz>. **1996**.
12. JPL Tools. JPL Small-Body Database Browser NASA, California Institute of Technology, Jet Propulsion Laboratory (JPL), JPL Small-Body Database Browser, Orbit Diagram https://ssd.jpl.nasa.gov/tools/sbdb_lookup.html#/?des=1P. **2023**.
13. Encrenaz, T.; Greathouse, T.K.; Richter, M.J.; Lacy, J.H.; Fouchet, T.; Bézard, B.; Lefèvre, F.; Forget, F.; Atreya, S.K. A stringent upper limit to SO₂ in the Martian atmosphere. *Astronomy & Astrophysics* **2011**, *530*, A37, doi:10.1051/0004-6361/201116820.

- 489 14. Flahaut, J.; Quantin, C.; Allemand, P.; Thomas, P.; Le Deit, L. Identification, distribution and possible origins of sulfates in
490 Capri Chasma (Mars), inferred from CRISM data. *Journal of Geophysical Research* **2010**, *115*, E11007,
491 doi:10.1029/2009JE003566.
- 492 15. Mangold, N.; Baratoux, D.; Witasse, O.; Encrenaz, T.; Sotin, C. Mars: a small terrestrial planet. *Astron Astrophys Rev* **2016**, *24*,
493 15, doi:10.1007/s00159-016-0099-5.
- 494 16. Kozyrev, N.A. Observation of a Volcanic Process on the Moon (in Russian). *Sky and Telescope* **1959**, 184-186.
- 495 17. Kozyrev, N.A. Physical Observations of the Lunar Surfaces. In *Physics and Astronomy of the Moon*, Kopal, Z., Ed. Academic
496 Press: New York and London, 1962; Vol. 4, pp. 385-404.
- 497 18. Dadaev, A.N. Nikolai A. Kozyrev (1908 –1983) - Discoverer of Lunar Volcanism. *Letters to Progress in Physics* **2009**, *3*, L1-L14.
- 498 19. Safronov, A.N. Theory of the Origin of Terrestrial and Lunar Ores. *International Journal of Geosciences* **2023**, *14*, 547-583,
499 doi:10.4236/ijg.2023.146030.
- 500 20. Brož, P.; Oehler, D.; Mazzini, A.; Hauber, E.; Komatsu, G.; Etioppe, G.; Cuřín, V. An overview of sedimentary volcanism on
501 Mars. *EGUshere Preprint* **2023**, 1-47, doi:10.5194/egusphere-2022-1458.
- 502 21. Ceylan, S.; Giardini, D.; Clinton, J.F.; Kim, D.; Khan, A.; Stähler, S.C.; Zenhäusern, G.; Lognonné, P.; Banerdt, W.B. Mapping
503 the seismicity of Mars with InSight. *Journal of Geophysical Research: Planets* **2023**, *128*, e2023JE007826,
504 doi:10.1029/2023JE007826.
- 505 22. Kim, D.; Stähler, S.C.; Ceylan, S.; Lekic, V.; Maguire, R.; Zenhäusern, G.; Clinton, J.; Giardini, D.; Khan, A.; Panning, M.P., et
506 al. Structure along the martian dichotomy constrained by Rayleigh and love waves and their overtones. *Geophysical Research*
507 *Letters* **2023**, *50*, e2022GL101666, doi:10.1029/2022GL101666.
- 508 23. Frey, H.V. Impact constraints on the age and origin of the lowlands of Mars. *Geophysical Research Letters* **2006**, *33*, L08S02,
509 doi:10.1029/2005GL024484.
- 510 24. Andrews-Hanna, J.C.; Zuber, M.T.; Banerdt, W.B. The Borealis basin and the origin of the martian crustal dichotomy. *Nature*
511 **2008**, *453*, 1212-1216, doi:10.1038/nature07011.
- 512 25. Marinova, M.M.; Aharonson, O.; Asphaug, E. Mega-impact formation of the Mars hemispheric dichotomy. *Nature* **2008**, *453*,
513 1216-1219, doi:10.1038/nature07070.
- 514 26. Safronov, A.N. The Basic Principles of Creation of Habitable Planets around Stars in the Milky Way Galaxy. *International*
515 *Journal of Astronomy and Astrophysics* **2016**, *6*, 512-554, doi:10.4236/ijaa.2016.64039.
- 516 27. Voronin, D.V. Computer Modeling of Planet Partial Fragmentation. *WSEAS Transactions on Fluid Mechanics* **2011**, *1*, 32-50.
- 517 28. de Meijer, R.J.; Anisichkin, V.F.; van Westrenen, W. () Forming the Moon from Terrestrial Silicate-Rich Material. *Chemical*
518 *Geology* **2013**, *345*, 40-49, doi:10.1016/j.chemgeo.2012.12.015.
- 519 29. Brandenburg, J.E. Evidence for Large Planetary Climate Altering Thermonuclear Explosions on Mars in the Past. *Internation-*
520 *al Journal of Astronomy and Astrophysics* **2023**, *13*, 112-139, doi:10.4236/ijaa.2023.132007.
- 521 30. Kuroda, P. Nuclear Fission in the Early History of the Earth. *Nature Astronomy* **1960**, *187*, 36-38, doi:10.1038/187036a0.
- 522 31. Herndon, J.M. Nuclear Fission Reactors as Energy Sources for the Giant Outer Planets. *Naturwissenschaften* **1992**, *79*, 7-14,
523 doi:10.1007/BF01132272.
- 524 32. Herndon, J.M. Feasibility of a Nuclear Fission Reactor at the Center of the Earth as the Energy Source for the Geomagnetic
525 Field. *Journal of Geomagnetism and Geoelectricity* **1993**, *45*, 423-437, doi:10.5636/jgg.45.423.
- 526 33. Hollenbach, D.F.; Herndon, J.M. Deep-Earth Reactor: Nuclear Fission, Helium, and the Geomagnetic Field. *Proceedings of the*
527 *National Academy of Sciences of the United States of America (PNAS)* **2001**, *98*, 11085-11090, doi:10.1073/pnas.201393998.
- 528 34. Herndon, J.M. Nuclear Georeactor Origin of Oceanic Basalt ³He/⁴He, Evidence, and Implications. *Proceedings of the National*
529 *Academy of Sciences of the International Journal of Geosciences United States of America (PNAS)* **2003**, *100*, 3047-3050,
530 doi:10.1073/pnas.0437778100.
- 531 35. Herndon, J.M. Terracentric Nuclear Fission Georeactor: Background, Basis, Feasibility, Structure, Evidence and Geophysical
532 Implications. *Current Science* **2014**, *106*, 528-541.
- 533 36. Villanueva, G.L.; Mumma, M.J.; Novak, R.E. A sensitive search for organics (CH₄, CH₃OH, H₂CO, C₂H₆, C₂H₂, C₂H₄), hy-
534 droperoxyl (HO₂), nitrogen compounds (N₂O, NH₃, HCN) and chlorine species (HCl, CH₃Cl) on Mars using ground-based
535 high resolution infrared spectroscopy. *Icarus* **2013**, *223*, 11–27, doi:10.1016/j.icarus.2012.11.013.
- 536 37. Lunine, J.I.; Chambers, J.; Morbidelli, A.; Leshin, L.A. The origin of water on Mars. *Icarus* **2003**, *165*, 1-8,
537 doi:10.1016/s0019-1035(03)00172-6
- 538 38. Lammer, H.; Selsis, F.; Penz, T.; Amerstorfer, U.V.; Lichtenegger, H.I.M.; Kolb, C.; Ribas, I. Atmospheric Evolution and the
539 History of Water on Mars. In *Water on Mars and Life. Advances in Astrobiology and Biogeophysics*, Springer: Berlin, Heidel-
540 berg, 2005; Vol. 4, pp. 25–43.

- 541 39. Marov, M.Y.; Ipatov, S.I. Delivery of Water and Volatiles to the Terrestrial Planets and the Moon. *Solar System Research* **2018**,
542 52, 392–400, doi:10.1134/S0038094618050052.
- 543 40. Alsaeed, N.R.; Jakosky, B.M. Mars Water and D/H Evolution from 3.3 Ga to Present. *Journal of Geophysical Research: Planets*
544 **2019**, 124, doi:10.1029/2019je006066
- 545 41. Nazari-Sharabian, M.; Aghababaei, M.; Karakouzian, M.; Karami, M. Water on Mars - A Literature Review *MDPI Galaxies*
546 **2020**, 8, 40, doi:10.3390/galaxies8020040.
- 547 42. Knapmeyer, M.; Stähler, S.C.; Daubar, I.; Forget, F.; Spiga, A.; Pierron, T.; van Driel, M.; Banfield, D.; Hauber, E.; Grott, M., et
548 al. Seasonal seismic activity on Mars. *Earth and Planetary Science Letters* **2021**, 576, 117-171, doi:10.1016/j.epsl.2021.117171.
- 549 43. Knapmeyer, M.; Stähler, S.C.; Daubar, I.; Forget, F.; Spiga, A.; Pierron, T.; van Driel, M.; Banfield, D.; Hauber, E.; Grott, M., et
550 al. Marsquake activity driven by the Sun? *52nd Lunar and Planetary Science Conference* **2021**, LPI Contrib. No. 2548, 1069.pdf.
- 551 44. Posiolova, L.V.; Lognonné, P.; Banerdt, W.B.; Clinton, J.; Collins, G.S.; Kawamura, T.; Ceylan, S.; Daubar, I.J.; Fernando, B.;
552 Froment, M., et al. Largest recent impact craters on Mars: Orbital imaging and surface seismic co-investigation. *Science* **2022**,
553 378, 412-417, doi:10.1126/science.abq7704.
- 554 45. Garcia, R.F.; Daubar, I.J.; Beucler, É.; Posiolova, L.V.; Collins, G.S.; Lognonné, P.; Rolland, L.; Xu, Z.; Wójcicka, N.; Spiga, A.,
555 et al. Newly formed craters on Mars located using seismic and acoustic wave data from InSight. *Nature Geoscience* **2022**, 15,
556 774-780, doi:10.1038/s41561-022-01014-0.
- 557 46. Fernando, B.; Daubar, I.J.; Charalambous, C.; Grindrod, P.M.; Stott, A.; Ateqi, A.A.; Atri, D.; Ceylan, S.; Clinton, J.; Fillingim,
558 M., et al. A Tectonic Origin for the Largest Marsquake Observed by InSight. *Geophysical Research Letters* **2023**, 50,
559 e2023GL103619, doi:10.1029/2023GL103619.
- 560 47. Lei, Z.; Jinhai, Z.; Ross, N.M.; Peng, C.; Jihang, L. A thermal origin for super-high-frequency marsquakes. *Icarus* **2023**, 390,
561 115327, doi:10.1016/j.icarus.2022.115327.
- 562 48. Burr, D.M.; Tanaka, K.L.; Yoshikawa, K. Pingos on Earth and Mars. *Planetary and Space Science* **2009**, 57, 541-555,
563 doi:10.1016/j.pss.2008.11.003.
- 564 49. Dundas, C.M.; McEwen, A.S. An assessment of evidence for pingos on Mars using HiRISE. *Icarus* **2010**, 205, 244-258,
565 doi:10.1016/j.icarus.2009.02.020.
- 566 50. Soare, R.J.; Conway, S.J.; Pearce, G.D.; Dohm, J.M.; Grindrod, P.M. Possible crater-based pingos, paleolakes and periglacial
567 landscapes at the high latitudes of Utopia Planitia, Mars. *Icarus* **2013**, 225, 971-981, doi:10.1016/j.icarus.2012.08.041.
- 568 51. Kawamura, T.; Clinton, J.F.; Zenhäusern, G.; Ceylan, S.; Horleston, A.C.; Dahmen, N.L.; Duran, C.; Kim, D.; Plasman, M.;
569 Stähler, S.C., et al. S1222a - The Largest Marsquake Detected by InSight. *Geophysical Research Letters* **2022**, 50, e2022GL101543,
570 doi:10.1029/2022GL101543.
- 571 52. Chabris, C.; Simons, D. *The Invisible Gorilla: And Other Ways Our Intuitions Deceive Us*; Crown: New York, USA, 2011; pp. 320.
- 572 53. Böse, M.; et al. Magnitude Scales for Marsquakes Calibrated from InSight Data, BSSA. **2021**, doi:10.1785/0120210045.
- 573 54. Luger, R.; Sestovic, M.; Kruse, E.; Grimm, S.L.; Demory, B.-O.; Agol, E.; Bolmont, E.; Fabrycky, D.; Fernandes, C.S.; van
574 Grootel, V., et al. A seven-planet resonant chain in TRAPPIST-1. *Nature Astronomy* **2017**, 1, 0129, doi:10.1038/s41550-017-0129.
- 575 55. Leleu, A.; Y. Alibert; N. C. Hara; M. J. Hooton; T. G. Wilson; P. Robutel; J.-B. Delisle; J. Laskar; S. Hoyer; C. Lovis, et al. Six
576 transiting planets and a chain of Laplace resonances in TOI-178. *Astronomy & Astrophysics* **2021**, 649, A26
577 doi:10.1051/0004-6361/202039767.
- 578 56. Luque, R.; Osborn, H.P.; Leleu, A.; Pallé, E.; Bonfanti, A.; Barragán, O.; Wilson, T.G.; Broeg, C.; Cameron, A.C.; Lendl, M., et
579 al. A resonant sextuplet of sub-Neptunes transiting the bright star HD 110067. *Nature* **2023**, 623 932-936,
580 doi:10.1038/s41586-023-06692-3.
- 581 57. Cseh, J.; Dang, P.; Szilágyi, S.; Lévai, G. Orbital Regularity of Exoplanets and the Symmetries of the Kepler Problem. *MDPI*
582 *Symmetry* **2023**, 15, 2114, doi:10.3390/sym15122114.
- 583 58. Chang, H.-Y. Titius-Bode's Relation in Exoplanetary Systems. *Journal of Astronomy and Space Sciences* **2023**, 40, 67-77,
584 doi:10.5140/JASS.2023.40.2.67.
- 585 59. Gribbin, J. Planetary Alignments, Solar Activity and Climatic Change. *Nature* **1973**, 246, 453-454, doi:10.1038/246453a0.
- 586 60. Gribbin, J.R.; Plagemann, S.H. *The Jupiter Effect: The Planets as Triggers of Devastating Earthquakes*; Walker: New York, 1974.
- 587 61. Awadh, S.M. Solar system planetary alignment triggers tides and earthquakes. *Journal of Coastal Conservation* **2021** 25,
588 doi:10.1007/s11852-021-00822-7.
- 589 62. Okhlopkov, V.P. Relationship of Solar Activity Cycles to Planetary Configurations. *Bulletin of the Russian Academy of Sciences.*
590 *Physics* **2013**, 77, 599–601, doi:10.3103/S1062873813050420.
- 591 63. Okhlopkov, V.P. Cycles of solar activity and the configurations of the planets. *Journal of Physics: Conference Series* **2013** 409
592 012199, doi:10.1088/1742-6596/409/1/012199.

- 593 64. Okhlopkov, V.P. The 11-Year Cycle of Solar Activity and Configurations of the Planets. *Moscow University Physics Bulletin*
594 **2014**, *69*, 257–262, doi:10.3103/S0027134914030126.
- 595 65. Stefani, F.; Giesecke, A.; Weber, N.; Weier, T. Synchronized Helicity Oscillations: A Link between Planetary Tides and the
596 Solar Cycle? . *Solar Physics* **2016**, *291*, 2197–2212, doi:10.1007/s11207-016-0968-0.
- 597 66. Stefani, F.; Giesecke, A.; Weier, T. A Model of a Tidally Synchronized Solar Dynamo. *Solar Physics* **2019**, *294*, Article No. 60,
598 doi:10.1007/s11207-019-1447-1.
- 599 67. Nataf, H.-C. Tidally Synchronized Solar Dynamo: A Rebuttal. *Solar Physics* **2022**, *297*, 107, doi:10.1007/s11207-022-02038-w.
- 600 68. Scafetta, N. Comment on “Tidally Synchronized Solar Dynamo: A Rebuttal” by Nataf (Solar Phys. 297, 107, 2022). *Solar*
601 *Physics* **2023**, *298*, 24, doi:10.1007/s11207-023-02118-5.
- 602 69. Scafetta, N. The complex planetary synchronization structure of the solar system. *Pattern Recognition in Physics* **2014** *2*, 1-19,
603 doi:10.5194/prp-2-1-2014.
- 604 70. Scafetta, N.; Bianchini, A. The Planetary Theory of Solar Activity Variability: A Review. *Frontiers in Astronomy and Space*
605 *Sciences* **2022**, *9*, 937930, doi:10.3389/fspas.2022.937930.
- 606 71. Scafetta, N.; Bianchini, A. Overview of the Spectral Coherence between Planetary Resonances and Solar and Climate Oscilla-
607 tions. *Climate* **2023**, *11*, 77, doi:10.3390/cli11040077.
- 608 72. GWTC-3: Compact Binary Coalescences Observed by LIGO and Virgo during the Second Part of the Third Observing Run.
609 **2023**, arXiv:2111.03606, 1-88.
- 610 73. Riess, A.G., Anand, G.S., Yuan, W., Casertano, S., Dolphin, A., et al. Crowded No More: The Accuracy of the Hubble Con-
611 stant Tested with High-resolution Observations of Cepheids by JWST. *The Astrophysical Journal Letters*, **2024**, 956, L18,
612 doi:10.3847/2041-8213/acf769.
- 613 74. Oppenheim, J. and Russo, A. Anomalous contribution to galactic rotation curves due to stochastic spacetime. **2024**,
614 arXiv:2402.19459, 1-18.
- 615 75. Gupta, R.P. Testing CCC+TL Cosmology with Observed Baryon Acoustic Oscillation Features. *The Astrophysical Journal*,
616 **2024**, 964, 1-7, doi:10.3847/1538-4357/ad1bc6.
- 617 76. Safronov, A.N. Life Origin in the Milky Way Galaxy: I. The Stellar Nucleogenesis of Elements Necessary for the Life 718
618 Origin. *Journal of High Energy Physics, Gravitation and Cosmology*, **2024**, *10*, 647-680, doi:10.4236/jhepgc.2024.102040.
- 619
620
621